Evaluating the Traffic Functionality of Emergency Transportation Networks: Development of Reachability Indicators and a Decision-Support Tool for Tokyo

Toshihiro Osaragi
Institute of Science Tokyo
osaragi.t.20f7@m.isct.ac.jp

Maki Kishimoto
Institute of Science Tokyo
kishimoto.m.8408@m.isct.ac.jp

ABSTRACT

Ensuring the continuity of emergency transportation networks is essential for effective post-disaster response and recovery. This study develops a quantitative and policy-oriented evaluation framework to assess the traffic functionality of Tokyo's designated emergency transportation roads by integrating roadside building vulnerability data with seismic retrofit information. Two novel indicators—the Section Reachability Ratio and the Comprehensive Reachability Ratio—are introduced to quantify network accessibility under probabilistic road blockages caused by building collapse. Using Monte Carlo simulation, the framework estimates accessibility probabilities by coupling building-specific seismic performance data with the urban transportation network structure. The results reveal pronounced spatial heterogeneity in retrofit effects and identify segments where improvements in building seismic performance produce measurable gains in network robustness. A structural transition in reachability behavior is observed as accessibility requirements become more stringent, supporting the adoption of a robustness-oriented threshold definition. The study further presents a GIS-integrated evaluation application that operationalizes the proposed indicators within a real-world planning context. Rather than prescribing optimal retrofit decisions, the framework provides a transparent and empirically grounded basis for comparing alternative retrofit scenarios, thereby supporting evidence-based disaster mitigation planning and future optimization-oriented extensions.

Keywords

Emergency transportation roads, Seismic retrofitting, Traffic functionality, Network resilience, Decision support system.

INTRODUCTION

The continuity of emergency transportation networks is critical for post-disaster response and recovery. During the 1995 Hyogo-ken Nanbu Earthquake, the collapse of roadside buildings obstructed major arterial roads, significantly hindering emergency vehicle passage, relief supply delivery, and overall reconstruction efforts (Usui & Konagaya, 1995). In response, many local governments have promoted the seismic retrofitting, reconstruction, or removal of vulnerable roadside buildings. These efforts specifically aim to safeguard the functionality of designated emergency transportation roads—vital lifelines for firefighting, rescue operations, and emergency logistics during large-scale disasters.

To systematically accelerate these efforts, the Tokyo Metropolitan Government enacted the Ordinance for Promoting Seismic Retrofit of Buildings along Emergency Transportation Roads in March 2011 (hereafter "the Ordinance") (Tokyo Metropolitan Government, 2011). The Ordinance follows a structured six-component framework ((I)–(VI)). First (I), approximately 1,000 km of the 2,000 km emergency road network were designated as "specific emergency transportation roads" due to their critical need for roadside building reinforcement. The remaining segments are classified as "general emergency transportation roads." Figure 1 illustrates this network, comprising expressways and ordinary roads that form the skeletal structure of Tokyo's urban connectivity.

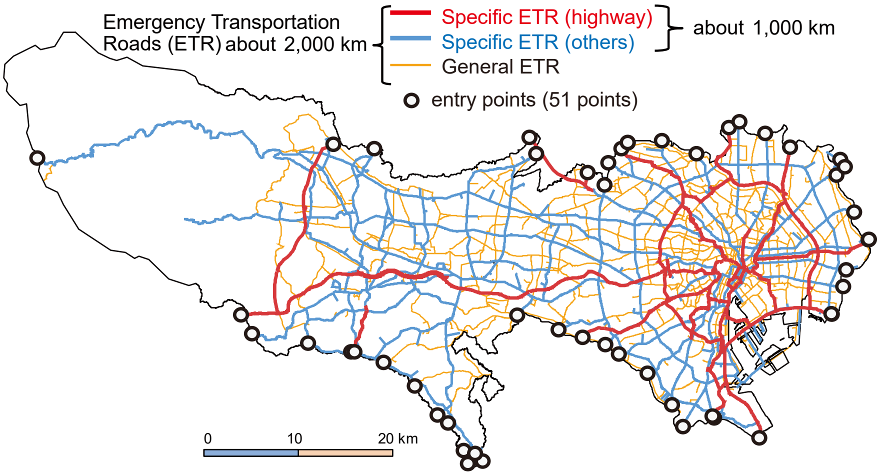

Figure 1. Emergency Transportation Roads and Access Points from Neighboring Prefectures to Tokyo

Second (II), buildings posing a high risk of obstructing these specific routes upon collapse are identified as "specific roadside buildings." As shown in Fig. 2, these are defined based on three criteria: (1) plots directly abutting a specific emergency transportation road; (2) construction prior to the May 1981 seismic code; and (3) height exceeding approximately half the width of the adjoining road. The designation accounts for various road geometries: for roads narrower than 12 m, buildings that could obstruct 6 m or more are designated (Fig. 2(a)); for wider roads, the threshold is the center line or median strip (Fig. 2(b)); and for elevated structures, the road surface is treated as ground level (Fig. 2(c)).

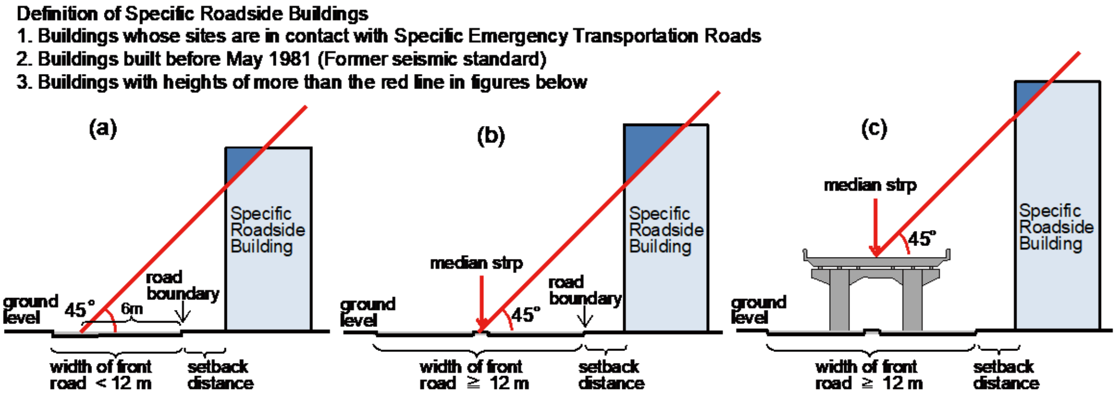

Figure 2. Definition of Specific Roadside Buildings

Under components (III) and (IV), owners of these buildings must report their seismic status and undergo mandatory seismic diagnosis. As of June 2025, of the 18,282 buildings along specific emergency roads, 4,829 were built under the old code. While 2,820 have been retrofitted, 1,938 remain unreinforced, and 71 have yet to undergo diagnosis despite legal requirements. To address this, the Ordinance stipulates that owners must endeavor to implement retrofitting (V), supported by subsidies from the Tokyo Metropolitan Government for diagnosis and construction (VI).

To date, the "seismic retrofitting rate" has been the primary indicator for monitoring progress. However, while simple to calculate, this rate fails to adequately represent the traffic functionality of the network. Although the number of collapsed buildings can be estimated statistically, the actual accessibility of road sections depends on the spatial configuration of blockages. Thus, traffic function is highly sensitive to both the spatial distribution of vulnerable buildings and the structural topology of the road network.

While Osaragi (2021) examined functionality via accessibility and travel efficiency from Tokyo's boundaries to 59 major disaster response bases, this provided only a partial evaluation as it did not account for accessibility to arbitrary points within the city. Therefore, this study proposes new indicators to evaluate the traffic functions of specific emergency transportation roads. We define the **Section Reachability Ratio** for individual road sections and the **Comprehensive Reachability Ratio** for area-wide assessment. Furthermore, we developed an original GIS-integrated application to simulate and visualize how seismic retrofitting impacts these ratios, providing a practical decision-support tool for data-driven spatial decision support system for function-oriented disaster mitigation planning.

RELATED PREVIOUS RESEARCH

The seismic performance and resilience of urban transportation networks have been extensively investigated, particularly concerning how earthquake-induced building damage leads to road blockages and disrupts emergency mobility. Early foundational work demonstrated that debris from collapsed buildings can severely restrict both short- and long-term accessibility (Goretti & Sarli, 2006). Complementing these approaches, Zolfaghari and Mogheisi (2012) presented one of the earliest probabilistic seismic damage assessments for urban transportation networks, highlighting the necessity of explicitly modeling uncertainty in road failure mechanisms. Building on this perspective, Hirokawa and Osaragi (2016) developed an integrated disaster simulation system incorporating models of building collapse, road blockage, and fire spread, providing an essential framework for understanding cascading urban disruptions.

Probabilistic methods for evaluating road accessibility have since become increasingly sophisticated. Li and Zhou (2020) employed Monte Carlo simulations to optimize seismic risk-mitigation investment strategies, while Hosseini et al. (2023) proposed methods to estimate debris-related blockages for recovery planning. Moratalla et al. (2023) extended these approaches to multi-hazard contexts, demonstrating that cascading risks significantly amplify accessibility losses. In regions with complex terrain, Sotiriadis et al. (2025) developed a tailored probabilistic framework for analyzing roadway functionality in mountainous urban areas. Furthermore, Nicolosi et al. (2022) advanced resilience evaluation within road asset management by integrating probabilistic damage estimation with restoration and cost modeling.

Parallel to these developments, resilience-oriented frameworks have gained significant attention. Kilanitis and Sextos (2019) proposed an integrated approach using fragility assessment and traffic assignment to quantify system-level resilience trajectories. In a metropolitan application, Alemdar (2025) utilized a GIS-based multi-criteria decision-making (MCDM) framework to assess seismic risk in Istanbul's transportation network. Recent advances in data availability have also bolstered this field; for instance, Civera et al. (2025) provided comprehensive datasets for infrastructure visualization and vulnerability assessment.

GIS-based methodologies have become central to analyzing transportation networks under natural hazards. Toma-Danila et al. (2020) introduced network-risk, an open-source GIS toolbox linking building-collapse probabilities with road blockage scenarios, which was later extended to a time-dependent framework for assessing emergency transport accessibility (Toma-Danila, 2022). Within the Japanese context, Osaragi (2021) demonstrated how roadside building vulnerability affects accessibility along designated emergency roads and quantified the functional benefits of seismic retrofitting.

A prominent research direction concerns the role of seismic retrofitting. El-Maissi et al. (2021) emphasized that structural retrofitting is central to reducing network exposure. Several studies suggest that interventions targeted at bottleneck segments yield disproportionately large improvements in overall functionality (Li & Zhou, 2020; Nicolosi et al., 2022; Osaragi, 2021). However, despite the acknowledged impact of roadside buildings on road blockages, most existing literature focuses primarily on bridges or roadway structures rather than the vulnerabilities of the built environment lining the road corridors.

Against this background, the present study makes four key contributions:

1. Probabilistic Integration: It integrates roadside building vulnerability and earthquake-induced debris blockage into a probabilistic framework for evaluating emergency transportation network functionality in a megacity.
2. Novel Metrics: It introduces two reachability-based indicators—the Section Reachability Ratio and the Comprehensive Reachability Ratio—to quantify accessibility under probabilistic blockage conditions.
3. Threshold Identification: It examines how seismic retrofitting influences network-level accessibility, revealing non-linear transition behavior and highlighting locations where targeted retrofits can substantially improve accessibility.
4. Operational Tooling: It develops a GIS-based decision-support application that operationalizes the proposed probabilistic framework for practical disaster mitigation and resilience planning.

INDICATORS FOR EVALUATING TRAFFIC FUNCTIONALITY

In general, the traffic functionality of a road network is considered "excellent" when it facilitates efficient and rapid access between any two arbitrary points. However, under disaster scenarios involving road blockages, a critical evaluative perspective is whether emergency vehicles entering from outside the affected area can reach any given location.

Therefore, this study evaluates traffic functionality by focusing on areas reachable by emergency vehicles entering from neighboring regions (specifically, entry points along the prefectural boundaries adjacent to Tokyo). It is important to acknowledge that the functionality of surrounding road networks may also be impaired; relying on a limited number of entry points could lead to an overly optimistic evaluation if those specific points become inaccessible due to damage in adjacent prefectures. Conversely, requiring simultaneous accessibility from all entry points might be overly conservative. Accordingly, this study determines reachability based on whether a road section can be accessed from more than half of the entry points. To determine an appropriate threshold for this criterion, a sensitivity analysis was conducted by varying the reachability threshold (i.e., the required number of accessible entry points). The results indicate that although absolute reachability values vary depending on the threshold, the relative effectiveness of seismic retrofitting strategies remains consistent across different thresholds (see Appendix A).

Figure 3 illustrates the conceptual framework for calculating the two proposed indicators: the Section Reachability Ratio and the Comprehensive Reachability Ratio. Figure 3(a) depicts four individual simulation runs. Road sections reachable from more than half of the entry points (segments between intersections or median strip openings) are shown in light blue, while unreachable segments are in black. The road section is defined as a continuous emergency transportation link between two designated network nodes (intersections or median strip openings) in the official road network dataset (Figure 3(b)). Entry points correspond to predefined access nodes connecting the emergency transportation network to surrounding arterial roads. Figure 3(c) overlays the results from these simulations to express the frequency with which each section was reachable.

This proportion is defined as the Section Reachability Ratio (S_j), which represents the probability that a given road section j is reachable. It is expressed mathematically as:

$$S_j = \frac{1}{K}\sum_{k=1}^{K}\frac{L_{jk}}{L_j} \qquad (1)$$

where:

- j: index of the road section
- k: index of the simulation run
- K: total number of simulation runs
- S_j: Section Reachability Ratio of road section j
- L_j: total length of road section j
- L_{jk}: length of the part of road section j reachable from more than half of the entry points in the k-th simulation.

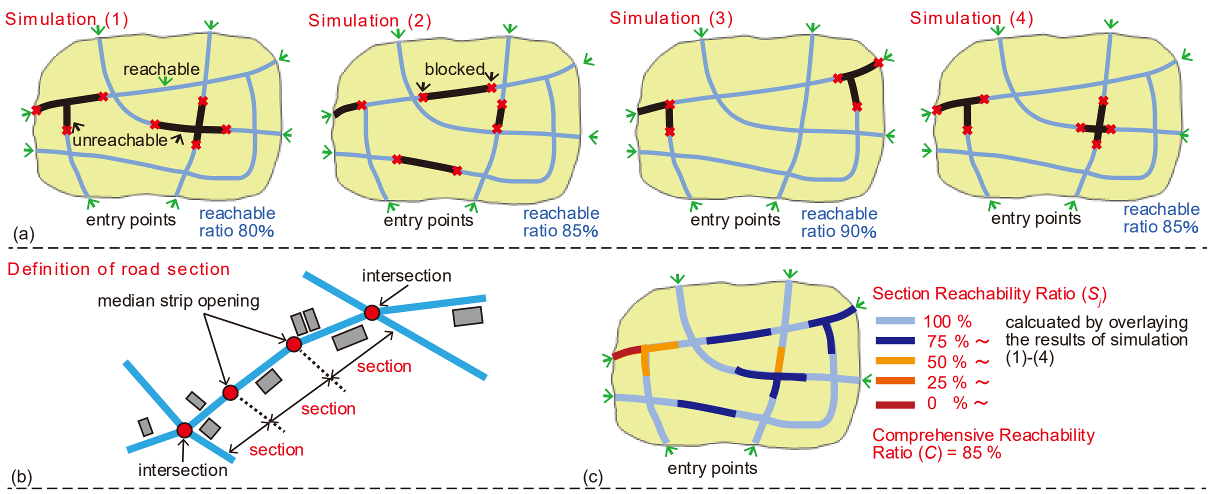

Figure 3. Conceptual Framework for Calculating Section and Comprehensive Reachability Ratios

When building collapses generate debris that partially obstructs a road section, the affected portion is identified as an unreachable sub-section. The Section Reachability Ratio is then computed based on the proportion of the section length that remains functionally traversable under the simulated damage scenario. In other words, reachability is not treated as a binary attribute of the entire section but rather as a length-based measure that reflects partial obstruction within the section.

For each simulation k, the ratio of the total length of reachable road sections to the total network length—termed the Reachable Ratio (R_k)—is calculated. The average of these values across all simulations is defined as the Comprehensive Reachability Ratio (C). This indicator represents the expected proportion of the entire road network that remains accessible, serving as a measure of overall system functionality. The Reachable Ratio (R_k) and Comprehensive Reachability Ratio (C) are expressed as follows:

$$R_k = \frac{\sum_{j=1}^{N} L_{jk}}{\sum_{j=1}^{N} L_j} \qquad (2)$$

$$C = \frac{1}{K}\sum_{k=1}^{K} R_k \qquad (3)$$

where:

R_k: Reachable Ratio for simulation k
C: Comprehensive Reachability Ratio
N: Total number of road sections

Section-level reachability metrics (the Section Reachability Ratio) provide detailed, location-specific information and are therefore highly informative for local-level planning and tactical decision-making. However, an aggregated metric (the Comprehensive Reachability Ratio) serves a distinct and complementary purpose at the strategic level. While section-level indicators allow planners to identify vulnerable road sections, they do not provide a system-wide assessment of overall emergency transportation performance. In large and administratively fragmented metropolitan areas—such as Tokyo, which consists of 62 local governments—a single aggregated metric enables higher-level authorities to evaluate overall network robustness, compare alternative policy scenarios, and establish measurable numerical targets. Importantly, the Comprehensive Reachability Ratio does not replace the section-level metric but rather complements it. The section-level metric captures spatial heterogeneity, whereas the aggregated metric provides a macroscopic measure of system-wide functional resilience. Although such aggregation inevitably reduces spatial detail, it enhances interpretability and comparability across policy alternatives. In practical applications of the proposed framework, both indicators are used in combination: the comprehensive indicator supports strategic target setting, while the section-level indicator helps identify priority locations for seismic retrofitting interventions.

SIMULATION SYSTEM FOR EVALUATING TRAFFIC FUNCTIONALITY

Building Collapse Model

Detailed data on the seismic performance of specific roadside buildings are available because seismic diagnosis is mandated by local ordinances. Among these data, the Seismic Index of Structure (*Is* value)—which accounts for structural strength, ductility, building morphology, and aging—is particularly useful. Generally, buildings with an *Is* value of 0.6 or higher are considered to possess sufficient seismic resistance (Ministry of Land, Infrastructure, Transport and Tourism, 2021). This study adopts the method proposed by Hayashi et al. (2000), which estimates the probability of building collapse based on *Is* values using damage ratio curves for reinforced concrete (RC) buildings derived from the 1995 Hyogo-ken Nanbu Earthquake.

In typical earthquake damage assessments, specific scenarios—such as the Northern Tokyo Bay Earthquake—are assumed. In these models, damage is concentrated near the epicenter, making the results highly dependent on the assumed seismic source. While randomizing the epicenter and averaging the outcomes is a common alternative, this approach risks underestimating localized catastrophic damage due to the smoothing effect of the averaging process.

To address this, this study does not assume a specific earthquake scenario or fixed epicenter. Instead, we assume uniform ground shaking across the entire study area. Referencing damage scenarios for major inland earthquakes where the intensity reaches "6-upper" on the Japan Meteorological Agency (JMA) scale, we assumed a measured seismic intensity of 6.2 (the midpoint of the 6-upper range) throughout Tokyo. Following the method of Tong et al. (1996), this intensity was converted to a Peak Ground Velocity (PGV) of 66 cm/s.

Figure 4 illustrates the building collapse probability function and the resulting relationship between the *Is* value and collapse probability. For each designated roadside building, the collapse probability was estimated using this function (for buildings with unknown status, the mean *Is* value of all buildings was applied). The actual collapse state in each simulation run was then determined by comparing the estimated probability with a uniformly distributed random number. The direction of debris from collapsed buildings is a critical factor for road obstruction. While longitudinal and transverse *Is* values would ideally be used to determine the direction of collapse, such detailed data were unavailable. Therefore, we assumed a 50% probability that debris affects the fronting road . For buildings located on street corners along designated emergency transport routes, a 50% probability was assigned to collapse toward either of the adjacent roads (see Appendix A). As shown in Fig. 4, since the collapse probability for buildings with $Is \geq 0.6$ is negligibly small, these buildings were assumed to remain intact.

$$P(i) = \Phi\left(\frac{\ln(PGV(i)) - \lambda(i)}{\zeta(i)}\right)$$

$$\lambda(i) = \ln\left(PGV_0 \frac{Is(i)}{Is_1}\right), \qquad \zeta(i) = \zeta_0$$

$P(i)$	: probability of building collapse of builbing i
Φ	: standarized normal distribution function
$PGV(i)$	: peak ground velocity on builbing i (cm/s)
$Is(i)$	: Is value of building i
$\lambda(i), \zeta$	: average and standard deviation of ln(PGV(i))
PGV_0, Is_1, ζ_0	: values used in analysis (250 cm/s, 0.4 cm/s, 0.6)

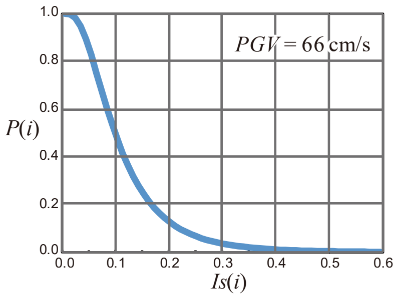

Figure 4. Relationship between Seismic Index of Structure (*Is*) and Building Collapse Probability

Road Blockage Model

During a major earthquake, road blockages can result from various types of physical damage, including the failure of elevated structures and bridge piers, liquefaction, pavement cracking, and the collapse of utility poles. Traffic congestion also significantly impedes accessibility. However, as this study specifically focuses on how the seismic performance of roadside buildings influences traffic functionality, only road blockages caused by building collapses are considered in the model.

Figure 5 presents a conceptual diagram of the road blockage model, illustrating how debris from collapsed buildings affects the passability of adjacent roadways. Given the thousands of designated buildings involved, it is impractical to model each structure individually. Therefore, we developed a simplified model consistent with the parameters defined in the Tokyo Metropolitan Ordinance (Tokyo Metropolitan Government, 2011).

When a building collapses, debris is assumed to scatter onto the adjacent roadway, with the extent of the debris increasing in proportion to the building's height. Most designated emergency transport routes are equipped with median strips; thus, if debris covers more than half the road width, one side of the carriageway is rendered completely impassable. The Ordinance defines "specific roadside buildings" partly based on a height threshold approximately equal to or greater than half the road width, implying that debris may reach a distance equivalent to the building's height.

The assumption that debris may extend up to the height of the collapsed building was not introduced as an arbitrary modeling choice. Rather, it is grounded in findings from post-earthquake field investigations conducted in Japan and is reflected in the criteria established by the Tokyo Metropolitan Ordinance (Tokyo Metropolitan Government, 2011) for identifying roadside buildings that may obstruct designated emergency transportation routes. Accordingly, this assumption functions as a regulatory boundary condition derived from empirically documented disaster behavior, rather than as a tunable analytical parameter within the simulation framework. The objective of the present study is to evaluate retrofit strategies under these empirically grounded and policy-relevant conditions, thereby ensuring consistency with actual disaster management planning practices in Tokyo. Nevertheless, it should be acknowledged that debris dispersion patterns may vary depending on structural failure modes or regional contexts. Application of the proposed framework to other jurisdictions would therefore require recalibration of such regulatory assumptions in accordance with locally observed disaster characteristics.

Even if one side of the road is obstructed, emergency vehicles may maintain mobility by utilizing the opposite lane (reverse-flow driving). Consequently, road functionality is not necessarily lost immediately. To evaluate emergency vehicle passability more accurately while remaining consistent with the Ordinance, this study introduces the concept of effective road width (x). The effective width after a building collapse is calculated as follows (Figure 5):

$$x = w + s - h \qquad (4)$$

where:

x: effective road width (m)
h: building height (m)
w: total road width (m)
s: setback distance from the road boundary (m)

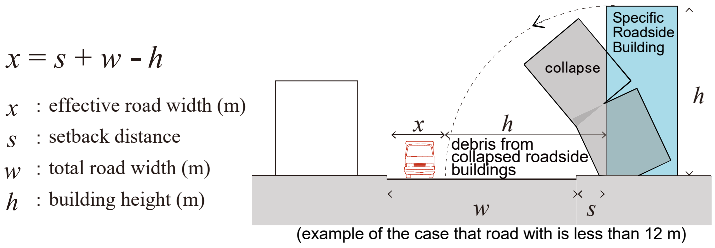

Figure 5. Calculation Method for Effective Road Width Following Building Collapse

In many conventional damage assessments, a road is considered impassable for emergency vehicles when $x < 4$ m. However, considering that other obstacles—such as abandoned vehicles—may further reduce the available space, we adopted a more conservative criterion: a road section is regarded as blocked when $x < 6$ m.

Furthermore, even if a single building collapse does not fully obstruct the road, the simultaneous collapse of two facing buildings can lead to a complete blockage. To account for this, pairs of opposing buildings (hereafter "building pairs") were pre-identified. A road section is judged as blocked if either a single building collapse results in $x < 6$ m or if both buildings in a pair collapse simultaneously.

The 6 m threshold was not introduced as a freely adjustable modeling parameter. Rather, it is explicitly grounded in the Tokyo Metropolitan Government's official disaster management guidelines, which are themselves informed by post-earthquake field investigations and consultations with emergency response experts. The 6 m criterion reflects operational requirements for large emergency vehicles under post-disaster conditions, taking into account maneuverability constraints as well as potential secondary obstacles such as debris or abandoned vehicles.

Although alternative thresholds could be considered under different regulatory or operational contexts, the purpose of the present study is not to explore arbitrary parameter variations but to evaluate retrofit strategies under empirically grounded and policy-relevant conditions. For this reason, the road-width assumption functions as a regulatory boundary condition rather than a tunable analytical parameter within the proposed framework. Application of the framework to other regions would therefore require recalibration of such regulatory parameters in accordance with local standards and disaster management practices.

Emergency Vehicle Model

To identify the road sections reachable by emergency vehicles entering from surrounding regions (prefectural boundaries), we developed an emergency vehicle movement model. In this model, the passability of the road network changes dynamically based on building collapse patterns. Furthermore, the presence of median dividers is explicitly modeled as a constraint on vehicle movement.

Under these considerations, the model assumes that emergency vehicles operate under the following conditions. The set of reachable road sections is then determined using a Breadth-First Search (BFS) algorithm:

1. Entry Points: Emergency vehicles enter the network from 51 designated entry points located along Tokyo's prefectural boundaries (see Figure 1).
2. Lane Utilization: Emergency vehicles are permitted to utilize the opposite lane (reverse-flow driving) to bypass obstructions within the same road section.
3. Median Constraints: Median dividers are treated as impassable barriers; vehicles cannot cross to the opposite side except at designated intersections or openings (see Figure 6).
4. Information Availability: All road blockage locations are assumed to be known in advance (perfect information), allowing for optimal pathfinding within the accessible network.

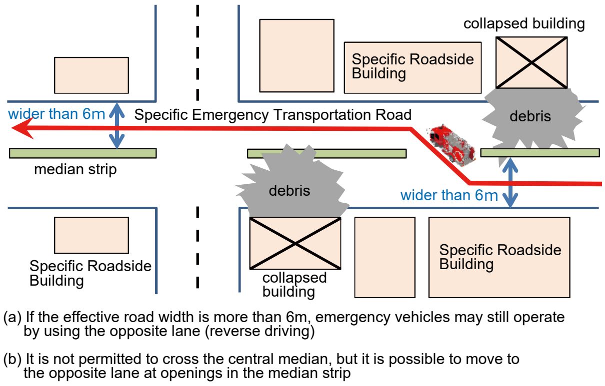

Figure 6. Conceptual Framework of the Vehicle Traffic Simulation

DATA AND SIMULATION CONDITIONS

Data Used

The road network for the designated emergency transportation roads was constructed using the Digital Map (Basic Geospatial Information) published by the Ministry of Land, Infrastructure, Transport and Tourism (MLIT), with supplementary road information added where necessary. The road link data were segmented into individual road sections, each attributed with physical characteristics such as road length and width. To ensure topological consistency, the network was structured so that expressways and non-expressways connect exclusively at designated interchanges.

For the designated roadside buildings, a comprehensive dataset was compiled from official seismic diagnosis and retrofitting reports. This dataset includes critical attributes for the simulation, such as:

- Building height and structural type
- Setback distance and the width of the fronting road
- Seismic Index of Structure (*Is* value)
- Construction year
- Identification of building pairs (opposing buildings on the same road section)

The Tokyo Metropolitan Government monitors seismic retrofit progress through biannual reviews. For this study, we utilized eight distinct datasets spanning from June 2019 to December 2022, allowing for a temporal analysis of how retrofitting progress influences network-level functionality.

Simulation Conditions

The simulations were executed according to the following iterative procedure:

1. Stochastic Building Collapse: For all designated roadside buildings with *Is* values below 0.6, the building collapse model was applied to determine the collapse state of each structure based on the assigned probabilities.
2. Road Blockage Estimation: The road blockage model was utilized to identify the specific locations of impassable road sections resulting from the building collapses determined in Step 1.
3. Reachability Extraction: Using the Breadth-First Search (BFS) algorithm, reachable and unreachable road sections were extracted relative to the 51 designated entry points along the prefectural boundaries.

A single execution of steps (1) through (3) constitutes one simulation run. Preliminary sensitivity analysis indicated that 10,000 simulation runs were necessary to achieve statistically stable outcomes. Consequently, for each of the eight time points in the dataset, 10,000 runs were performed to calculate the Section Reachability Ratio and the Comprehensive Reachability Ratio.

In each Monte Carlo iteration, collapse events are independently sampled for individual buildings according to their assigned collapse probabilities, and road obstructions are subsequently determined based on the simulated debris impact. Consequently, the simulation samples from the underlying probability distribution of potential damage scenarios rather than attempting a combinatorial enumeration of all possible blockage configurations.

To address concerns regarding statistical stability, a convergence analysis was conducted by progressively increasing the number of simulation runs and examining the resulting reachability metrics. The results indicate that the estimated values of both the Section Reachability Ratio and the Comprehensive Reachability Ratio stabilize beyond approximately 10,000 iterations, with only negligible variation in the mean values.

It should be emphasized that Monte Carlo simulation is designed to approximate the expected behavior of complex stochastic systems by sampling from the underlying probability distribution. The objective of the proposed framework is therefore not to deterministically evaluate every possible damage configuration, which would be computationally infeasible for a large urban network such as Tokyo, but rather to estimate the expected level of network functionality under probabilistic earthquake damage scenarios.

Estimation Results of Section and Comprehensive Reachability Ratios

Figures 7(a) and 7(b) illustrate the spatial distribution of the Section Reachability Ratio as of December 2022. The results indicate that expressways within the designated emergency transport network exhibit high reachability, with values exceeding 95%. In contrast, several non-expressway sections show significantly lower accessibility, with ratios falling below 60%.

Figures 7(c) and 7(d) present the temporal changes in the Section Reachability Ratio between June 2019 and December 2022. During this period, 198 roadside buildings were reported to have upgraded their *Is* values to 0.6 or higher. Consequently, the Comprehensive Reachability Ratio improved from 91.2% to 92.6%, representing a 1.4-percentage-point increase in overall network functionality.

Furthermore, several road sections exhibited substantial improvements in their individual Section Reachability Ratios. These findings demonstrate that the seismic retrofitting of roadside buildings directly enhances the traffic functionality of emergency transport routes, providing a measurable impact on urban resilience.

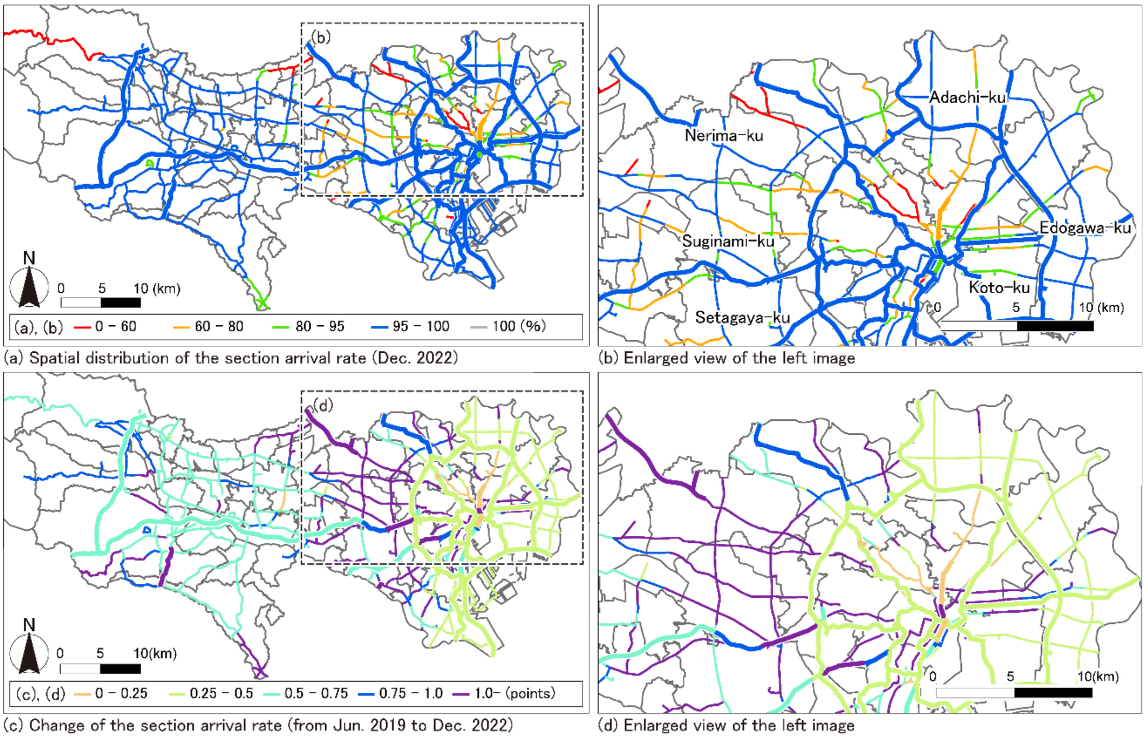

(a) Spatial distribution of the section arrival rate (Dec. 2022)
(b) Enlarged view of the left image
(c) Change of the section arrival rate (from Jun. 2019 to Dec. 2022)
(d) Enlarged view of the left image

Figure 7. Spatial Distribution and Temporal Change of Section Reachability Ratio (Thick lines: expressways; thin lines: non-expressways)

DEVELOPMENT OF A SEISMIC RETROFIT EVALUATION APPLICATION

Effectiveness of the Simulation for Decision Support

Previous research on the decision-making processes of building owners regarding seismic retrofitting has emphasized that raising disaster awareness and providing accessible information are critical for promoting structural improvements (Koshiyama et al., 2006). To encourage active cooperation from owners, it is effective to communicate not only the seismic risks inherent to the building itself but also the broader societal consequences—specifically, how a building's potential collapse could impair the traffic functionality of the surrounding road network. Visualizing these impacts can facilitate a shared understanding of the necessity for retrofitting.

Simultaneously, for local governments tasked with developing and implementing seismic retrofit promotion plans, providing evidence-based explanations regarding the expected benefits of these interventions is essential. Given constraints on time and budget, planners must accurately assess current network functionality and pre-evaluate the anticipated gains from specific retrofitting strategies to ensure efficient resource allocation. While the ultimate goal remains the complete seismic reinforcement of all designated roadside buildings, this is a long-term endeavor that requires the prioritization of specific buildings or routes.

Several studies have analyzed the effectiveness of prioritized retrofitting by constructing scenarios based on construction year or seismic performance and comparing their disaster mitigation effects (Yoshimura & Meguro, 2002). These studies demonstrated that prioritizing older structures is effective and that implementing phased retrofitting—dividing a single-stage process into multiple manageable phases—can reduce the financial and psychological burden on owners (Osaragi, 2021).

However, earlier research has rarely focused on identifying the specific buildings whose retrofitting directly contributes most to improving overall traffic functionality. Consequently, there is a clear need for a method to easily and quantitatively evaluate the degree to which the reinforcement of a specific structure enhances road network accessibility.

Seismic Retrofit Evaluation Application

Due to the complex interconnections within road networks, the seismic retrofitting of a single building can influence the reachability not only of the immediate road section but also of the surrounding area. Conversely, retrofitting multiple buildings may yield only marginal improvements in overall accessibility if they do not address critical bottlenecks. Figure 8 provides a simplified numerical example illustrating these effects, demonstrating why traffic functionality cannot be adequately assessed based solely on the aggregate seismic retrofit rate.

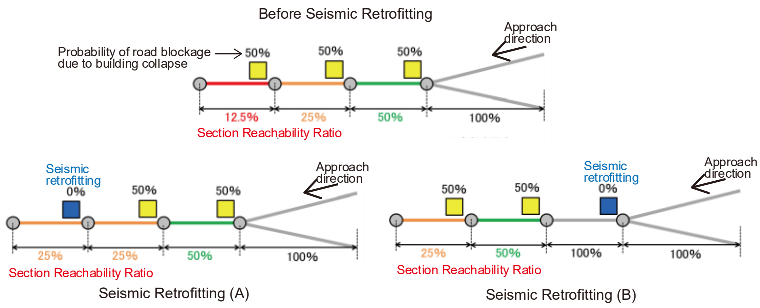

Figure 8. Conceptual Changes in Section Reachability Ratio Due to Seismic Retrofitting

To address these complexities and ensure practical applicability, we developed a specialized evaluation application (hereafter referred to as the Evaluation App) that operationalizes the proposed reachability indicators within a policy-oriented decision-support environment. The overall architecture of the Evaluation App is illustrated in Figure 9. The system translates retrofit assumptions into probabilistic network performance metrics through a structured three-mode workflow.

Input Data Creation Mode: Users select one or more roadside buildings for seismic retrofitting and assign post-retrofit structural performance values (Is values). These selections are saved as an external scenario file representing a specific retrofit policy configuration, which serves as the input to the simulation engine.

Simulation Execution Mode: Using the scenario file, the application performs Monte Carlo–based probabilistic simulations. Building-specific collapse probabilities are updated according to the assigned Is values, and potential debris impacts are generated under the regulatory assumptions described in the previous sections. The resulting road blockages are then propagated through the transportation network model to calculate the Section Reachability Ratio and the Comprehensive Reachability Ratio.

Output Data Review Mode: Simulation results are visualized spatially within a GIS-based interface. Users can examine the distribution of Section Reachability Ratios across individual road sections as well as the aggregated Comprehensive Reachability Ratio for the entire study area. The system also supports comparisons among multiple retrofit scenarios to facilitate policy evaluation.

By integrating these components, the Evaluation App enables policymakers and local administrators to quantitatively assess how alternative retrofit strategies influence emergency transportation performance under earthquake scenarios. Importantly, the system provides a structured link between building-level interventions and network-level resilience outcomes, thereby supporting evidence-based prioritization of limited retrofit resources.

The Evaluation App was implemented in C# and is designed for use by the 62 wards, cities, towns, and villages in Tokyo, allowing local governments to evaluate seismic retrofitting policies within their jurisdictions. The interface was intentionally designed to remain usable for officials without advanced GIS expertise while maintaining transparency in the underlying simulation logic. Although the present paper focuses primarily on the methodological formulation of the reachability indicators, the Evaluation App demonstrates their operational feasibility within a real-world planning context. A detailed software engineering description is beyond the scope of this study.

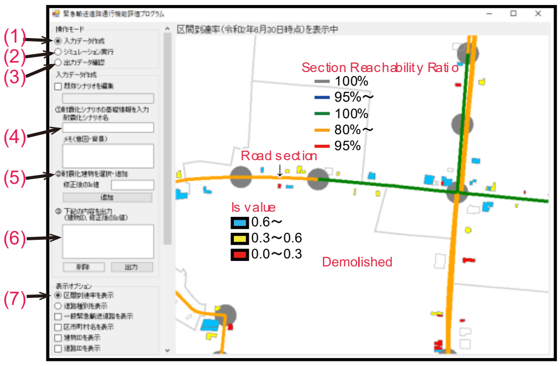

The main menu of the Evaluation App consists of the following components:
(1) Scenario Creation Mode – Mode for creating retrofit scenarios by selecting target buildings and assigning post-retrofit seismic performance values.
(2) Simulation Execution Mode – Mode for executing Monte Carlo simulations using the selected retrofit scenario.
(3) Output Data Review Mode – Mode for visualizing and reviewing simulation results, including the spatial distribution of Section Reachability Ratios and the Comprehensive Reachability Ratio.
(4) Input Scenario Name – Field for specifying and saving the name of the retrofit scenario.
(5) Input Target Buildings – Interface for selecting roadside buildings to be included in the retrofit scenario.
(6) List of Buildings to be Seismically Retrofitted – Panel displaying the buildings selected for seismic retrofitting in the current scenario.
(7) Drawing Options – Controls for adjusting map display settings and visualization layers.

Figure 9. Overview and Operational Workflow of the Traffic Function Evaluation App

DISCUSSION ON THE USEFULNESS OF THE EVALUATION APPLICATION

Distribution of the Evaluation Application to Municipal Governments in Tokyo

Officials responsible for developing municipal seismic retrofit promotion plans across Tokyo's wards and cities have consistently expressed a need to pre-evaluate the potential effectiveness of various retrofitting strategies. To meet this demand, the Evaluation App was distributed to local governments throughout Tokyo, and municipal staff were invited to pilot the system. As of March 2021, execution logs were collected from 12 separate wards and cities.

In the following analysis, we examine the execution logs from eight municipalities that actively utilized the application for their planning processes. To ensure temporal consistency across the different jurisdictions, the analysis was conducted using a standardized building dataset as of December 2020.

Examples of Application Use by Municipalities

Analysis of the execution logs revealed that the retrofit scenarios developed by the municipalities could be classified into five distinct types (A–E), each reflecting specific planning objectives.

Scenario (A): Full retrofitting within the municipality's jurisdiction. This scenario involves retrofitting all designated roadside buildings with $Is < 0.6$ within the local government's boundaries. It aims to estimate the maximum improvement in traffic functionality achievable through independent municipal effort. Five municipalities tested this scenario. The results indicated that even with a 100% internal retrofit rate, road sections with low reachability may persist if vulnerable buildings remain in adjacent jurisdictions (Figure 10). This finding underscores the necessity for neighboring municipalities to share data and coordinate strategies across administrative boundaries when developing seismic retrofit promotion plans.

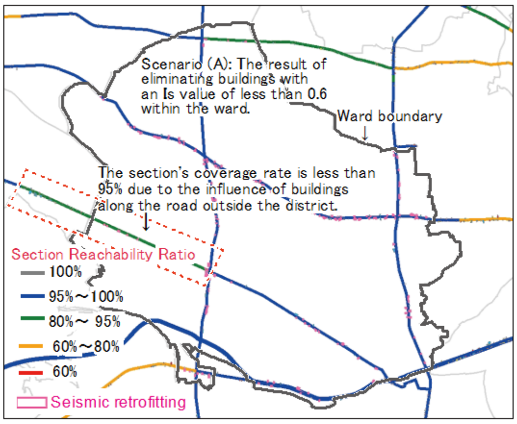

Figure 10. Visualization of Localized vs. Systematic Reachability Using the Evaluation App

Scenario (B): Retrofitting all buildings outside the municipality's jurisdiction. This scenario assesses the extent to which internal traffic functionality weaknesses are attributable to vulnerabilities in surrounding administrative areas. The Evaluation App enables the calculation of the Comprehensive Reachability Ratio on a per-municipality basis. Specifically, Equation (2) is applied using only the road network segments within the target municipality's territory.

Figure 11 presents the results of Scenario (B) for 53 municipalities, categorized into four groups:

- Group A: Already exhibit high reachability; external retrofitting pushes their ratios near 100%.
- Group B: Currently have low ratios but show significant improvement (e.g., from 70% to over 95%) when neighboring areas progress.
- Group C: Experience moderate improvement from external retrofits but still require substantial internal efforts.
- Group D: Show minimal improvement under Scenario (B), indicating that internal retrofitting initiatives are the primary critical requirement for these jurisdictions.

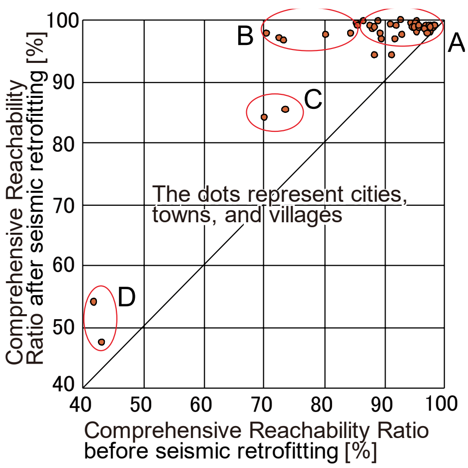

Figure 11. Impact on Comprehensive Reachability Ratios via External (Out-of-Jurisdiction) Retrofitting

Scenario (C): Targeted individual building retrofitting. In this scenario, planners evaluate how retrofitting specific, high-priority buildings affects the local network. Municipalities with fewer vulnerable buildings utilized this building-by-building approach to develop precise, evidence-based reinforcement strategies for notable structures.

Scenario (D): Corridor-based retrofitting. This scenario assesses the efficiency of prioritizing specific road corridors. Municipalities with a high density of seismically weak buildings utilized this to identify which arterial routes should be prioritized to maximize the effectiveness of their implementation plans.

Scenario (E): Prioritizing highly vulnerable buildings (*Is* < 0.3). This explores the functional gains from addressing only the most fragile structures first. While prioritizing buildings with high collapse probabilities is generally efficient (Osaragi, 2021), the spatial network structure dictates the actual outcome. This scenario allows for a quantitative assessment of the initial progress achievable by targeting the most critical structural risks.

The retrofit scenarios considered in this study are defined based on seismic performance thresholds used in Japanese retrofit policy. The seismic performance thresholds used in the scenarios are based on established engineering and policy standards in Japan. In particular, an Is value of 0.6 or higher is widely recognized, based on post-earthquake damage investigations, as a level at which the probability of building collapse becomes extremely low (Figure 4). This threshold is therefore adopted in national and metropolitan seismic retrofit guidelines as a target level for structural safety.

The intermediate threshold of Is ≥ 0.3 reflects the phased retrofit policy implemented by the Tokyo Metropolitan Government. Because upgrading a building directly to Is ≥ 0.6 can impose substantial financial burdens on building owners, the metropolitan government provides subsidy programs that support incremental seismic improvements. Under this policy framework, buildings can first be strengthened to Is ≥ 0.3 as an intermediate stage before achieving the final safety target of Is ≥ 0.6.

Accordingly, the scenarios examined in this study reflect realistic retrofit policy options currently considered in practice, allowing the simulation results to be interpreted within an actual planning context.

mprovement Effects by Road Corridor

As an application of Scenario (D), we analyzed Ward A and Ward B to examine the functional benefits of corridor-based retrofitting for designated roadside buildings. Using the execution logs provided by these municipalities, the target corridors and candidate buildings for retrofitting were identified and are summarized in Figure 12(a).

(a) The number of specific roadside buildings and the Is values for each route

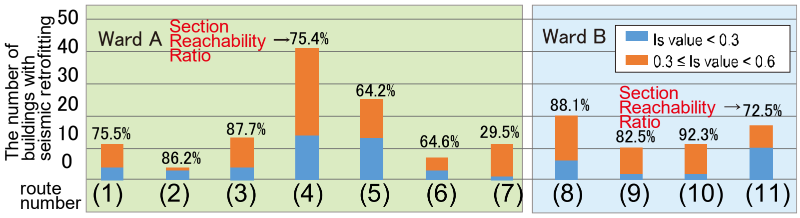

(b) Scenarios of seismic retrofitting

- Condition 1: Seismic retrofitting of buildings with Is value of less than 0.6 to achieve Is value of 0.6
- Condition 2: Seismic retrofitting of buildings with Is value of less than 0.3 to achieve Is value of 0.6
- Condition 3: Seismic retrofitting of buildings with Is value of less than 0.3 to achieve Is value of 0.3 (partial retrofitting)

Figure 12. Identification of Target Corridors and Retrofitting Scenarios

Since corridor-based strategies require the segmentation of the road network, both Ward A and Ward B developed their scenarios by categorizing roads based on their common names and evaluating each segment independently.

The Comprehensive Reachability Ratio is intended as a system-level performance indicator rather than a direct measure of cost-effectiveness. While Condition 1 (full retrofitting to Is ≥ 0.6) yields the largest improvement in network accessibility, it also entails higher implementation costs. The purpose of presenting multiple conditions is therefore to illustrate the trade-off between incremental seismic strengthening and improvements in network-level robustness. A comprehensive cost–benefit analysis of retrofit prioritization is beyond the scope of the present study; however, developing such an optimization-based evaluation framework represents an important direction for future research.

Figure 13 presents the relationship between the number of retrofitted buildings and the resulting Comprehensive Reachability Ratio. The baseline scenario is represented by the red line (Dec. 2020) in Figure 13, which reflects the existing building stock condition without additional retrofitting. By comparing simulation outcomes with this reference state, improvements in the Comprehensive Reachability Ratio can be interpreted as marginal gains relative to the current level of network robustness.

For Condition 1, where all buildings with *Is* < 0.6 were reinforced (see Figure 12(b)). The results reveal substantial variation in the "improvement efficiency" (the gain in reachability per retrofitted building) across different corridors. For example, along Corridor (2), retrofitting only five buildings improved the Comprehensive Reachability Ratio by 0.09 points. This single-corridor intervention accounted for 45.0% of the total improvement achieved by retrofitting 38 buildings across the entire area during the preceding six months (June–December 2020), demonstrating remarkably high efficiency.

Although the magnitude of change appears small (on the order of tenths of a percent), such changes correspond to meaningful improvements in a metropolitan-scale network such as Tokyo's. Given the size and density of the designated emergency transportation network, even a 0.1% increase in the Comprehensive Reachability Ratio may correspond to several additional road sections remaining accessible under disaster conditions.

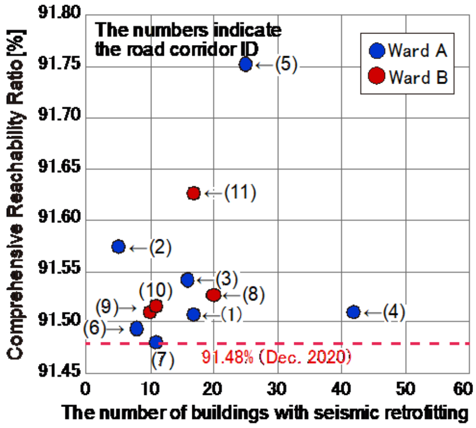

Figure 13. Relationship between Number of Retrofitted Buildings and Comprehensive Reachability Ratio

Furthermore, prioritizing specific buildings along each corridor can further enhance traffic functionality. As illustrated in Figure 14, for Corridor (11), retrofitting only the most vulnerable buildings (*Is* < 0.3) under Condition 2 and 3 yielded an improvement comparable to that of Condition 1. These findings highlight the strategic value of selective, risk-based retrofitting along key routes to maximize urban resilience under budgetary or time constraints.

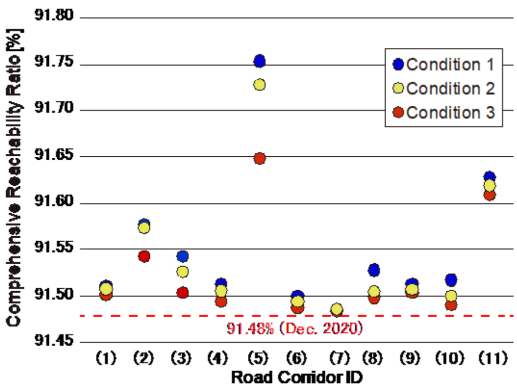

Figure 14. Impact of Targeted Section-based Retrofitting Scenarios on Comprehensive Reachability

DISCUSSION

Positioning of the Proposed Indicators

The primary objective of this study is to establish measurable and policy-relevant indicators that quantify the accessibility of emergency transportation networks under probabilistic earthquake scenarios. The Section Reachability Ratio and the Comprehensive Reachability Ratio are designed as evaluation metrics that translate building-level seismic performance into network-level functionality. It is important to emphasize that the proposed framework is descriptive in nature: it evaluates the expected performance of the transportation network under specified regulatory and probabilistic assumptions. The indicators provide a structured means of assessing how alternative seismic retrofitting configurations influence network robustness, but they do not, by themselves, prescribe optimal retrofit decisions. In this sense, the proposed indicators constitute a foundational analytical layer, providing measurable objective functions that can support more advanced decision-support models.

Toward a Prescriptive Optimization Framework

Seismic retrofitting under budget constraints can naturally be formulated as a resource allocation problem. Decision makers may seek to maximize network accessibility subject to financial limitations, heterogeneous retrofit costs, and administrative constraints. The indicators proposed in this study can serve directly as objective functions in such an optimization framework. For example, maximizing the Comprehensive Reachability Ratio under a budget constraint would enable the prioritization of retrofitting actions that produce the greatest improvement in network robustness.

However, incorporating budget constraints and heterogeneous cost structures introduces substantial combinatorial complexity. A full-scale optimization model would require the integration of building-specific retrofit costs, varying improvement levels in *Is* values, probabilistic collapse behavior, and the propagation of road blockages through the transportation network. Developing and computationally implementing such a prescriptive optimization model is beyond the scope of the present paper. Nevertheless, the analytical framework proposed here provides the quantitative foundation upon which such models can be constructed.

Interpretation and Scope of Model Assumptions

The modeling assumptions adopted in this study—such as debris dispersion distance and the required road width for emergency vehicle passage—are not introduced as freely adjustable parameters. Rather, they are grounded in post-earthquake field investigations and reflected in the Tokyo Metropolitan Government's regulatory standards for emergency transportation planning. Accordingly, the proposed framework evaluates retrofit strategies under empirically grounded and policy-defined boundary conditions.

The purpose of the model is therefore not to conduct exhaustive parametric sensitivity analyses, but to provide a consistent and interpretable evaluation tool aligned with actual planning practice. Although alternative assumptions could change the absolute values of the reachability indicators, the relative comparison of retrofit scenarios remains structurally meaningful as long as consistent regulatory conditions are maintained.

Limitations

Several limitations should be acknowledged. First, the model assumes probabilistic independence in building collapse simulations and does not explicitly represent correlated structural failures or cascading infrastructure disruptions. Second, debris dispersion and road clearance conditions are represented using regulatory assumptions rather than detailed physical simulations of structural collapse processes. Third, accessibility from prefectural boundary entry points is treated as given, although transportation disruptions may also occur in adjacent jurisdictions. Finally, the present study does not explicitly incorporate economic costs into the analytical framework. As discussed above, integrating budget constraints and heterogeneous retrofit costs represents a natural extension toward a prescriptive decision-support model.

SUMMARY AND CONCLUSIONS

This study introduced two quantitative indicators—the Section Reachability Ratio and the Comprehensive Reachability Ratio—to evaluate the traffic functionality of designated emergency transportation roads under earthquake-induced damage scenarios. By integrating a probabilistic building collapse model, a road blockage model grounded in empirically documented disaster behavior, and an emergency vehicle movement model, we constructed a simulation-based evaluation framework that links building-level seismic performance to network-level accessibility.

The proposed indicators were formally defined using a spatially explicit representation of road sections and entry points, enabling systematic evaluation of network accessibility under probabilistic damage conditions. Application of the framework to Tokyo's designated emergency transportation network demonstrated that spatial disparities in roadside seismic retrofitting produce measurable differences in systemic accessibility. The analysis further revealed a structural transition in reachability behavior as accessibility requirements become more stringent, supporting the adoption of a robustness-oriented threshold definition based on majority entry-point accessibility.

To enhance practical applicability, a GIS-integrated Evaluation App was developed to operationalize the proposed indicators within a policy planning environment. The application enables municipal officials to translate alternative retrofit scenarios into quantitative network performance measures, thereby facilitating transparent comparison of policy options. Through pilot use by several municipalities in Tokyo, the system demonstrated its ability to support corridor-based prioritization and scenario-based planning for seismic retrofit promotion.

It is important to emphasize that the proposed framework is designed as an evaluation methodology rather than a prescriptive optimization model. The indicators provide a measurable analytical basis for assessing how retrofit actions influence network robustness, but they do not directly determine optimal retrofit strategies. Instead, they define objective performance metrics that can support the development of more advanced decision-support models.

Several limitations should also be acknowledged. The analysis relies on regulatory and empirically grounded assumptions regarding debris dispersion and emergency vehicle passability, and the simulation framework does not explicitly model correlated structural failures or inter-regional disruptions. In addition, retrofit costs are not incorporated directly into the analytical model.

Future research may extend the framework by integrating explicit budget constraints, incorporating economic cost heterogeneity, and modeling inter-regional infrastructure disruptions. Further methodological development may also explore optimization-based retrofit prioritization using the proposed reachability indicators as objective functions.

By establishing a transparent and structurally grounded methodology for evaluating emergency transportation functionality, this study contributes to bridging structural vulnerability analysis and metropolitan-scale disaster mitigation planning, providing a quantitative basis for evidence-based seismic retrofit policy design.

ACKNOWLEDGMENTS

This paper is based on discussions conducted within the Tokyo Metropolitan Government Seismic Retrofit Promotion Plan Review Committee and was compiled under the responsibility of one of its members, Toshihiro Osaragi. The authors express sincere appreciation to the members of the committee, the officials of the Tokyo Metropolitan Government Bureau of Urban Development, and the municipal officers who provided execution logs from the Evaluation App. This paper is a substantially revised and expanded version of Osaragi and Kishimoto (2019).

REFERENCES

Alemdar, K.D. (2025). Seismic risk assessment of transportation networks for the impending Istanbul earthquake with GIS-based MCDM approach. *Nat Hazards, 121*, 10085–10123. https://doi.org/10.1007/s11069-025-07199-y

Civera, M., Aloschi, F., Di Maio, G.M. et al. (2025). Seismic resilience of urban networks: dataset for infrastructure visualization and vulnerability assessment. *Sci Data*, *12*, 1614. https://doi.org/10.1038/s41597-025-05903-y

El-Maissi, A. M., Argyroudis, S. A., & Nazri, F. M. (2021). Seismic Vulnerability Assessment Methodologies for Roadway Assets and Networks: A State-of-the-Art Review. *Sustainability*, *13*(1), 61. https://doi.org/10.3390/su13010061

Goretti, A., & Sarli, V. (2006). Road Network and Damaged Buildings in Urban Areas: Short and Long-term Interaction. *Bull Earthquake Eng*., *4*, 159–175. https://doi.org/10.1007/s10518-006-9004-3

Hayashi, Y., Suzuki, Y., Miyakoshi, J., & Watanabe, M. (2000). Seismic Risk Evaluation of Existing RC Buildings Based on Seismic Performance Indices, *Journal of Social Safety Science*, *2*, 235-242 (in Japanese)

Hirokawa, N., & Osaragi, T. (2016). Earthquake Disaster Simulation System: Integration of Models for

Building Collapse, Road Blockage, and Fire Spread, *Journal of Disaster Research* (*Special Issue on Disaster and Big Data* 1), *11*(2), 175-187. https://doi.org/10.20965/jdr.2016.p0175

Hosseini, Y., Mohammadi, R.K., & Yang, T.Y. (2023). Resource-based seismic resilience optimization of the blocked urban road network in emergency response phase considering uncertainties, *International Journal of Disaster Risk Reduction*, *85*. https://doi.org/10.1016/j.ijdrr.2022.103496

Kilanitis, I., & Sextos, A. (2019). Integrated seismic risk and resilience assessment of roadway networks in earthquake prone areas. *Bull Earthquake Eng.*, *17*, 181–210. https://doi.org/10.1007/s10518-018-0457-y

Kohiyama, M., Yoshimura, M., & Meguro, K. (2006). Incentives and Disincentives to Retrofitting: Importance of risk communication in programs of earthquake disaster reduction, *Journal of Environmental Engineering* (*Transactions of AIJ)*, *71*(606), 89-96. (in Japanese) https://doi.org/10.3130/aije.71.89_2

Li, J., & Zhou, Y. (2020). Optimizing risk mitigation investment strategies for improving post-earthquake road network resilience, *International Journal of Transportation Science and Technology*, *9*(4), 277-286. https://doi.org/10.1016/j.ijtst.2020.01.005

Moratalla, J.M., & Uma, S.R. (2023). Probabilistic assessment of road accessibility under cascading hazards, *International Journal of Disaster Risk Reduction*, *91*. https://doi.org/10.1016/j.ijdrr.2023.103692

Ministry of Land, Infrastructure and Transport (2021). https://www.mlit.go.jp/jutakukentiku/build/content/001470933.pdf (accessed 2023.8.23) (in Japanese)

Nicolosi, V., Augeri, M., D'Apuzzo, M. et al. (2022) A Probabilistic Approach to the Evaluation of Seismic Resilience in Road Asset Management. *Int J Disaster Risk Sci.*, *13*, 114–124. https://doi.org/10.1007/s13753-022-00395-5

Osaragi, T. (2021). Accessibility Evaluation of Specific Emergency Transportation Roads and Benefits of Seismic Retrofits on Buildings Adjoining Roads, *CoRe Paper – Analytical Modeling and Simulation Proceedings of the 17th ISCRAM Conference* – Blacksburg, VA, USA May 2020 Amanda Lee Hughes, Fiona McNeill and Christopher Zobel, eds., 143-156.

Osaragi, T., & Kishimoto, M. (2019). Accessibility Evaluation of Specific Emergency Transportation Roads and Effects of Quake-Resistant-Conversion of Roadside Buildings, *Journal of Architecture and Planning* (*Transactions of AIJ*), *84*(764), 2175-2182. https://doi.org/10.3130/aija.84.2175

Sotiriadis, D., Klimis, N., Margaris, B., Koutsoupaki, E.-I., Petala, E., & Dokas, I. (2025). Probabilistic seismic risk analysis of urban road networks in mountainous areas. In *Proceedings of The Challenges of Disaster Planning, Management, and Resilience* (*Chapter 6*). Nova Publishers.

Tokyo Metropolitan Government (2011). *Regulation to Promote Seismic Retrofit of Buildings along the Emergency Transportation Roads*. https://www.taishin.metro.tokyo.jp/tokyo/topic03.html (accessed 2023.8.23) (in Japanese)

Tokyo Metropolitan Government (2021). *Promoting the Seismic Resistance of Buildings*. https://www.taishin.metro.tokyo.jp/pdf/tokyo/r03_sokushinkeikaku_2.pdf (accessed 2026.3.1) (in Japanese)

Tokyo Metropolitan Government (2023). *Seismic Status of Buildings along the Specific Emergency Transportation Roads* (*As of the end of Jun. 2023*). https://www.taishin.metro.tokyo.lg.jp/tokyo/topic04_0506.html (accessed 2026.3.1) (in Japanese)

Toma-Danila, D., Armas, I., & Tiganescu, A. (2020). Network-risk: An open GIS toolbox for estimating the implications of transportation network damage due to natural hazards, tested for Bucharest, Romania. *Natural Hazards and Earth System Sciences*, *20*(5), 1421–1439. https://doi.org/10.5194/nhess-20-1421-2020

Toma-Danila, D. (2022). A time-dependent framework for analyzing emergency transport network accessibility after earthquakes. *Front. Earth Sci.*, *11 February 2022, Sec. Geohazards and Georisks, 10*. https://doi.org/10.3389/feart.2022.834052

Tong, H., & Yamazaki, F. (1996). Relationship between Ground Motion Indices and New JMA Seismic Intensity, *Seisan Kenkyu*, *48*(11), 31-34. (in Japanese)

Usui, T., & Konagaya, K. (1995). The Distribution Pattern of Debris in the Hansin-Awaji Earthquake: A GIS Analysis, *Geographical Review of Japan, Ser. A, Chirigaku Hyoron*, *68*(9), 621-633. https://doi.org/10.4157/grj1984a.68.9_621

Yoshimura, M., & Meguro, K. (2022). Evaluation of Financial Support System for Retrofitting of Existing Houses Based on Reduction in Governmental Expenses, *Journal of Social Safety Science*, *4*, 247-254. (in Japanese) https://doi.org/10.11314/jisss.4.247

Zolfaghari, M. R., & Mogheisi, M. (2012). Probabilistic Seismic Damage Assessment for Urban Transportation Network. *In Proceedings of the 15th World Conference on Earthquake Engineering* (WCEE 2012).

APPENDIX A: RATIONALE FOR THE MAJORITY-BASED REACHABILITY THRESHOLD

When evaluating accessibility to a given destination, two alternative definitions are considered: (1) reachability defined by accessibility from an arbitrary entry point, (2) reachability defined by accessibility from a majority of entry points (i.e., more than half of the entry points). The difference between these two approaches is clarified below.

In both cases, a sufficiently large number of simulations (denoted by K) are executed to evaluate whether an emergency vehicle entering from entry point i can reach the destination. One simulation trial is defined as executing the reachability test once from each entry point. Let δ_i^k be a dummy variable that takes the value 1 if the destination is reachable from entry point i in the k-th simulation, and 0 otherwise.

Let m^k denote the number of entry points from which the destination is reachable in the k-th simulation, and let n_i denote the number of successful reachability outcomes from entry point i across all simulations. These variables are expressed as:

$$m^k = \sum_{i=1}^{M} \delta_i^k \qquad \text{(A-1)}$$

$$n_i = \sum_{k=1}^{K} \delta_i^k \qquad \text{(A-2)}$$

These quantities can be organized as illustrated in Fig. A-1(a), where simulation outcomes are ordered in ascending order of m^k. Let a denote the number of simulations in which $m^k \leq m^*$, and b denote the number of simulations in which $m^k > m^*$. Under these definitions, reachability proportion under definition (1) (arbitrary entry-point reachability), denoted P, and the proportion under (2) (reachability from more than m^* entry points), denoted R, are expressed as:

$$P = \frac{1}{KM} \sum_{k=1}^{K} \sum_{i=1}^{M} \delta_i^k \qquad \text{(A-3)}$$

$$R = \frac{b}{K} \qquad \text{(A-4)}$$

Definition (1) represents the expected reachability rate calculated over all entry points and all simulation trials, effectively treating each entry-point simulation as an independent reachability observation, resulting in a total of $K \times M$ evaluations (where M is the number of entry points). While mathematically simple and intuitively understandable, this approach may smooth out trials in which m^k is small by averaging them with trials in which m^k is large. As evident from Eq. (A-3), this averaging process may obscure scenarios characterized by limited redundancy. Moreover, this definition does not explicitly account for the possibility that accessibility from certain entry points may depend on damage conditions in adjacent jurisdictions.

In contrast, definition (2) evaluates accessibility from the perspective of redundancy. Trials in which m^k is small are regarded as insufficient to ensure robust traffic functionality and are therefore excluded from being considered "reachable." Only when the destination is reachable from more than a specified threshold m^* entry points is the transportation function regarded as adequately secured. This approach is based on K simulation trials rather than $K \times M$ individual reachability evaluations and explicitly incorporates a redundancy requirement.

Considering the characteristics of both definitions, this study adopts definition (2). A remaining issue is how to determine the threshold value m^*. Additionally, we examine how variations in the probability that debris affects the fronting road influence the results. To examine this, we conducted simulations using the 59 large-scale rescue and emergency activity bases analyzed in our previous study as destinations (Osaragi, 2019). By varying m^*, we calculated both the frequency distribution of m^k and the corresponding value of R (Eq. A-4). The results exhibit the structural characteristics shown in Figure A-1(b)–(d).

As expected, a substantial number of simulation trials yielded small values of m^k, indicating limited redundancy; from a robustness perspective, such trials should not be regarded as sufficiently secure. On the other hand, as m^k approaches the total number of entry points M, the frequency of such outcomes decreases sharply.

Although it is difficult to derive a unique theoretical value for m^*, accessibility from more than half of the entry points provides a reasonable level of redundancy in the emergency transportation network. Accordingly, the threshold was set to $m^* = M/2$, which is equivalent to requiring accessibility from more than half of the entry points.

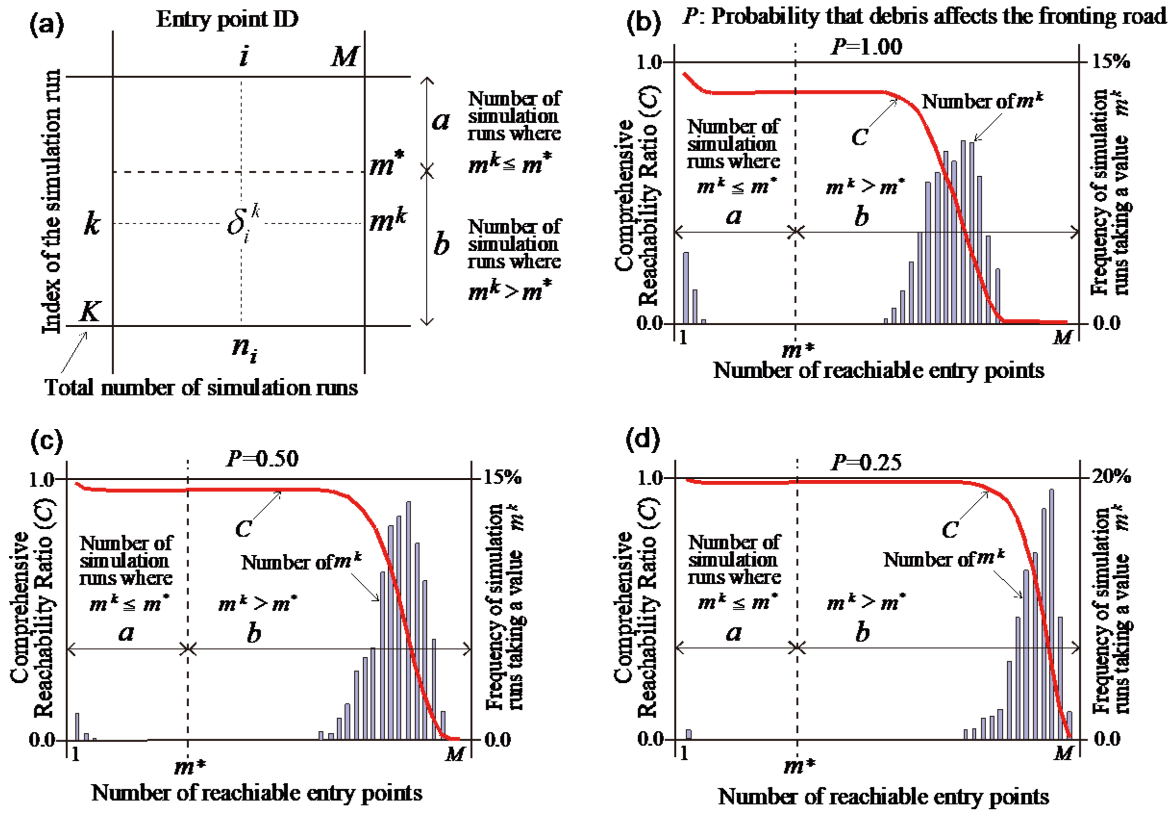

Figure A-1. Conceptual explanation and empirical distribution of reachable entry points: (a) Conceptual representation of simulation outcomes ordered by the number of reachable entry points m^k. (b)–(d) Frequency distributions of m^k and the corresponding value of the reachability proportion R under different threshold values m^*. The results illustrate that trials with small m^k occur frequently, whereas cases approaching the total number of entry points M are rare. This structural property supports the adoption of a majority-based reachability threshold.